Supplemental material

David et al., https://doi.org/10.1083/jcb.201805044

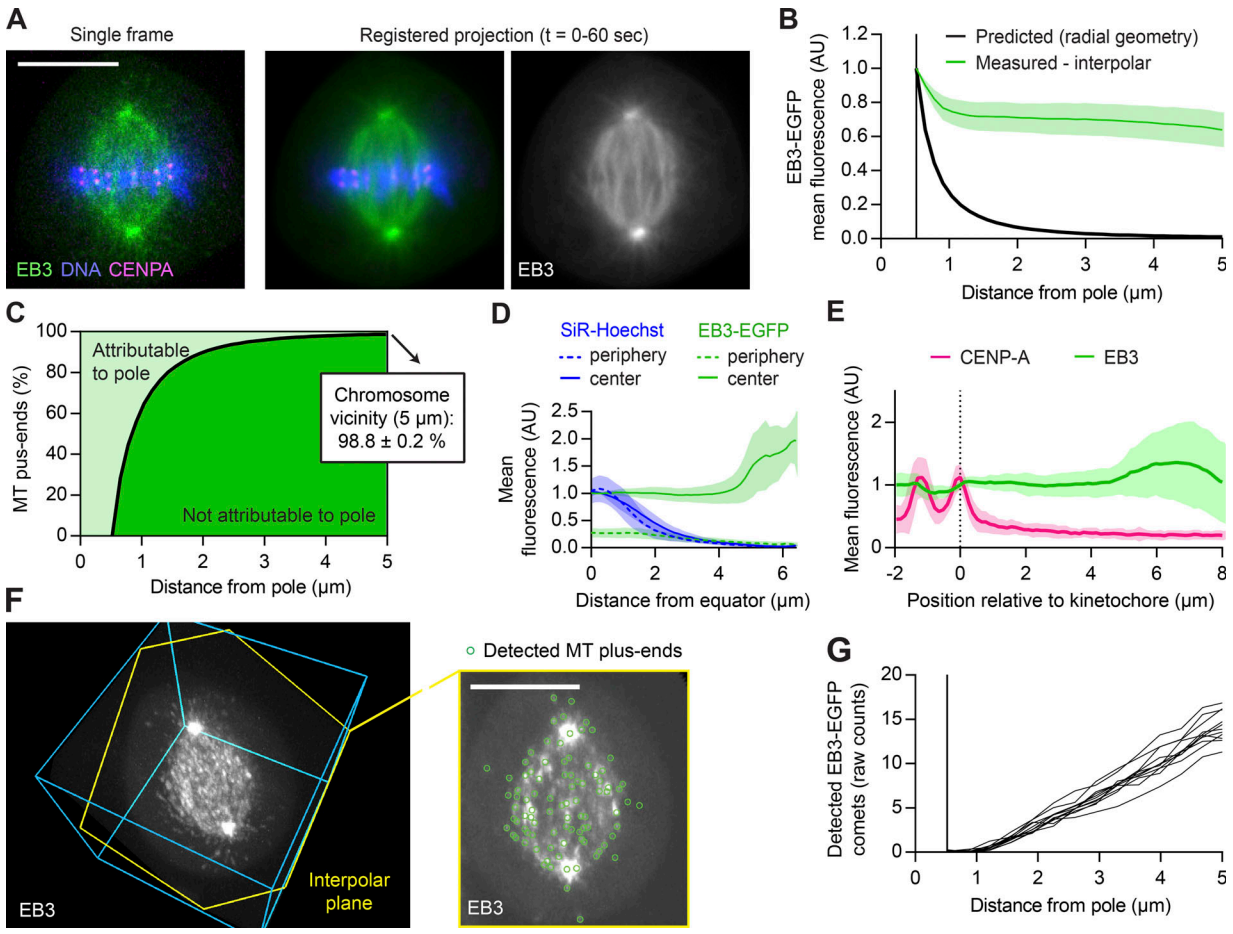

Figure S1. **Additional characterization of MT plus end distributions in unperturbed metaphase spindles. (A, B, D, and E)** Live-cell confocal microscopy of hTERT-RPE1 cells expressing EB3-EGFP (green) and mCherry-CENPA (magenta), stained with SiR-Hoechst (blue). **(A)** 1-min time-lapse videos were acquired during metaphase at 2 s/frame (see Video 2), registered to correct for spindle rotation (see Materials and methods for details) and projected to obtain mean-intensity images for analysis of MT plus end distributions. **(B)** Mean EB3-EGFP fluorescence intensity quantified in the projections thus obtained as in Fig. 1 (B and C). Black line indicates predicted signal dilution by radial geometry. (n = 25 cells, individual measurements normalized to centrosome rim). **(C)** Fractions of MT plus ends attributable (light green) and not attributable (dark green) to nucleation at the spindle poles in HeLa metaphase spindles. Computed from the measurements shown in Fig. 1 C as detailed in Materials and methods. **(D)** Mean EB3-EGFP and SiR-Hoechst fluorescence measured across the chromosome–cytoplasm boundary as described in Fig. 1 (D and E; n = 25 cells). **(E)** Mean EB3-EGFP and mCherry-CENPA fluorescence along curved lines connecting pairs of sister KTs to one of the spindle poles. Quantified as described in Fig. 1 (F and G; n = 49 profiles in 8 cells). **(F)** Automated 3D detection of MT plus ends in EB3-EGFP images. The slice highlighted in yellow follows the plane defined by the spindle poles and a random KT. **(G)** Quantification of detected MT plus ends at increasing distances from the nearest spindle pole. Plotted are the mean plus end numbers per video frame for each cell (n = 11 cells). Lines and shaded areas denote mean ± SD, respectively. Scale bars, 10 µm. AU, arbitrary units.

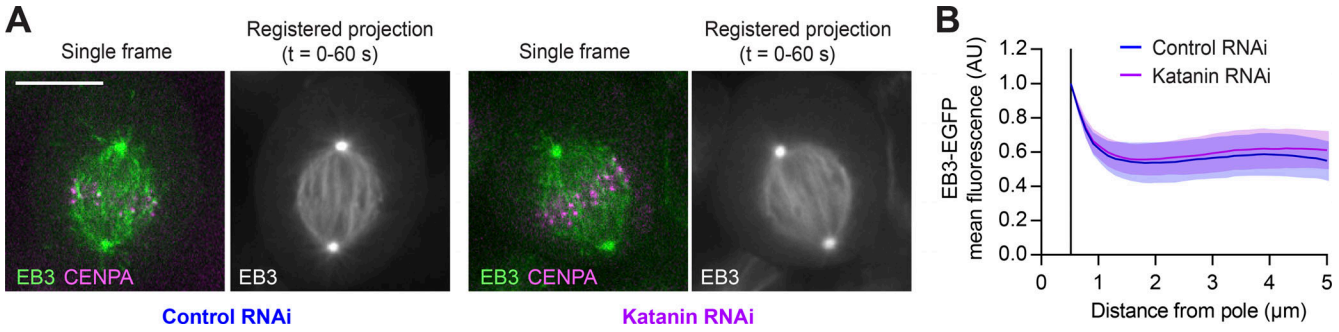

Figure S2. **MT plus end distribution in spindles of Katanin RNAi cells.** EB3-EGFP and mCherry-CENPA-expressing HeLa cells transfected with control or Katanin-targeting siRNAs (*n* = 14 and 18 cells, respectively). **(A)** Cells imaged during metaphase by live-cell confocal microscopy, for 1 min at 1 s/frame. Scale bar, 10 µm. **(B)** Mean EB3-EGFP fluorescence intensity quantified in average-intensity projections of registered time-lapse videos, as described in Fig. 1 (B and C). Lines and shaded areas denote mean ± SD, respectively. AU, arbitrary units.

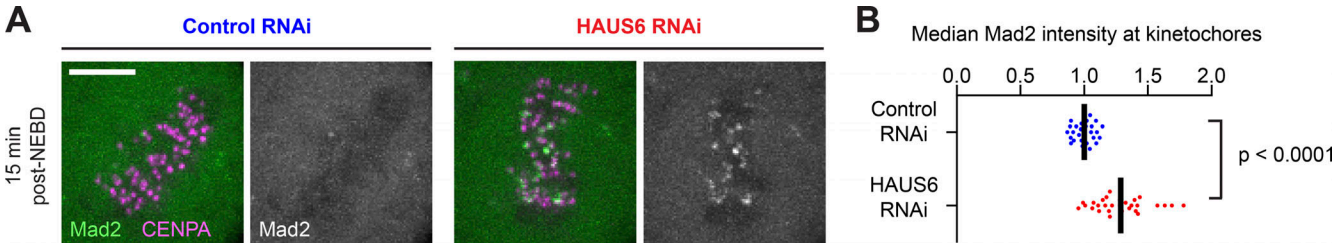

Figure S3. **Chromosome attachment defects in HAUS6 RNAi cells.** Live-cell microscopy of Mad2-EGFP– and mCherry-CENPA–expressing cells 48 h after transfection with control or HAUS6-targeting siRNAs (29 cells per condition, collected in three independent experiments). **(A)** 3D confocal stacks of mitotic cells were acquired 15 min after nuclear envelope breakdown (NEBD). Shown are representative maximum-intensity projections. Scale bar, 5 µm. **(B)** Mad2-EGFP intensities were quantified on mCherry-labeled KTs and normalized to cytoplasmic levels. Each data point plotted is the median value measured in one cell; bars denote mean of all cells. Distributions were compared not assuming normality using a Kolmogorov–Smirnov test.

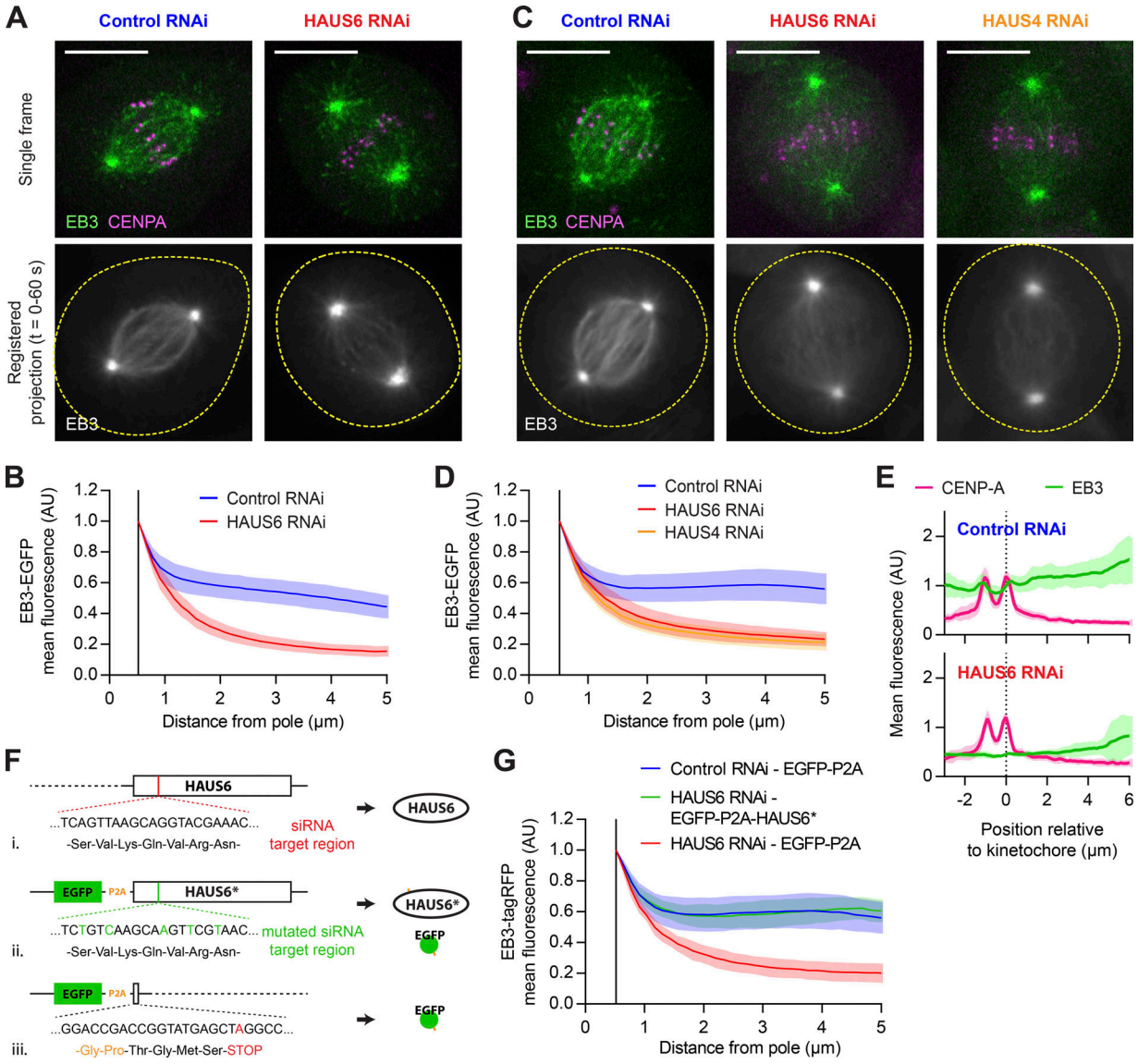

Figure S4. **Additional characterization of MT plus end distributions in HAUS6 RNAi spindles. (A–E)** Live-cell confocal microscopy of EB3-EGFP– and mCherry-CENPA–expressing cells. **(A and B)** hTERT-RPE1 cells transfected with control or HAUS6-targeting siRNAs (n = 34 and 31 cells, respectively, collected in three independent experiments). **(C–E)** HeLa cells transfected with control, HAUS4-targeting or HAUS6-targeting siRNAs (n = 33, 34, and 36 cells, respectively, collected in three independent experiments). **(A and C)** 1-min confocal time-lapse videos were acquired during metaphase at 2 s/frame. The dashed yellow lines indicate cell boundaries. Scale bars, 10 µm. **(B and D)** Mean EB3-EGFP fluorescence intensity quantified in average-intensity projections of registered time-lapse videos, as described in Fig. 1 (B and C). **(E)** Mean EB3-EGFP and mCherry-CENPA fluorescence along curved lines connecting pairs of sister KTs to one of the spindle poles. Quantified as described in Fig. 1 (F and G; n = 29 and 22 profiles for control and HAUS6 RNAi cells, respectively, in seven cells per condition). **(F and G)** EB3-tagRFP–expressing cells were transfected with control or HAUS6-targeting siRNAs. **(F)** Plasmids encoding for EGFP-P2A-HAUS6* (Fii, for expression of siRNA-resistant HAUS6) or EGFP-P2A (Fiii, control) were delivered 24 h later. See Materials and methods for details. **(G)** 48 h after siRNA transfection, cells were imaged during metaphase as in A and C. Mean EB3-tagRFP fluorescence was measured in EGFP-positive cells as described in Fig. 1 (B and C; n = 7, 10, and 5 cells for control RNAi-EGFP-P2A, HAUS6 RNAi-EFP-P2A-AUS6*, and HAUS6 RNAi-EGFP-P2A, respectively). Lines and shaded areas denote mean ± SD, respectively. AU, arbitrary units.

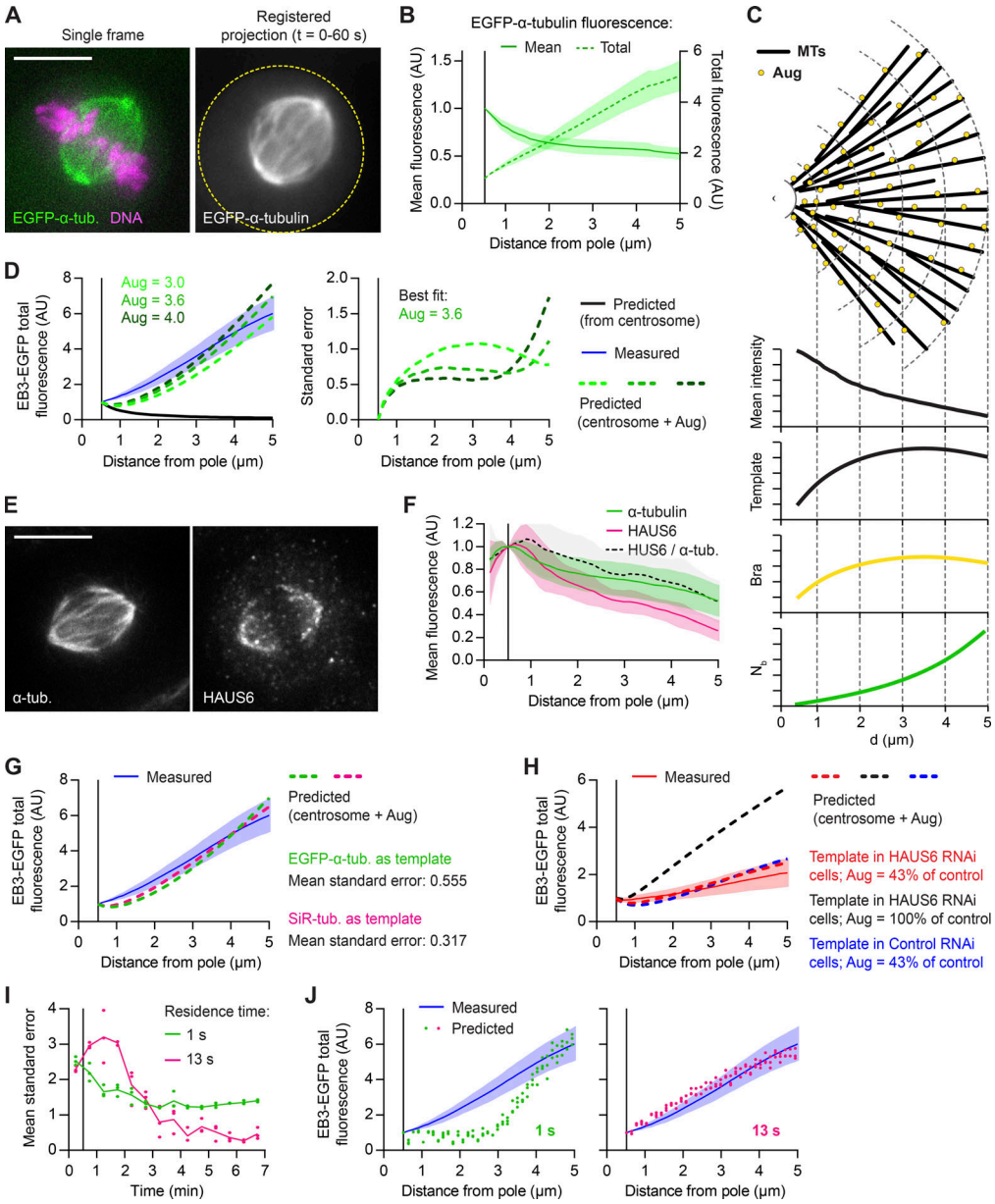

Figure S5. **Mathematical modeling of MT amplification in the metaphase spindle. (A and B)** Live-cell microscopy of HeLa cells expressing EGFP-α-tubulin (green) and H2b-mCherry (magenta). **(A)** 1-min time-lapse videos were acquired during metaphase at 2 s/frame, registered to correct for spindle rotation and projected to obtain mean-intensity images for analysis of MT lattice distributions. The dashed yellow line denotes the cell boundary. **(B)** Mean and total EGFP-α-tubulin fluorescence quantified in interpolar spindle regions as in Fig. 1 B. **(C)** Schematic representation of a model for uniform amplification of a template MT network. MT branching factors (Aug) distribute across MT lattices and generate plus ends at a fixed rate. The frequency distribution of MT-dependent plus end generation (Bra) is thus set to be a linear function of template distribution (Template), which is inferred from the mean fluorescence intensity of a MT marker (measured as in A and B). The number of MT plus ends generated on MT lattices (N_b) is a function of the branching frequency distribution Bra. For a prediction of MT plus end distributions, N_b is added to the number of plus ends originating at the spindle poles. See Materials and methods for details. **(D)** Three separate mathematical simulations wherein the template network measured in B is amplified using the indicated amplification parameters (Aug). The predicted MT plus end distribution is compared with the total EB3-EGFP fluorescence measured in Fig. 1 (A–C, left). The standard error of each prediction is plotted against distance from pole (right). **(E)** HAUS6 and α-tubulin or visualized by immunofluorescence in metaphase spindles of HeLa cells. **(F)** For data in E, mean fluorescence intensities were quantified in interpolar regions as in Fig. 1 (B and C; *n* = 34 cells in two independent experiments). **(G and H)** Mathematical predictions of MT template amplification. The predicted totals of MT plus ends are compared with the total EB3-EGFP fluorescence profiles measured in Fig. 1 (B and C; G) or in Fig. 4 E (H). **(G)** The measured fluorescence of the indicated MT markers (plotted in Fig. 3 F) was used to estimate MT template distributions. **(H)** The SiR-tubulin fluorescence measured in Fig. 4 C (in control or HAUS6 RNAi cells, as indicated) was used to estimate MT template distributions. **(I and J)** Computational simulations of MT amplification in a dynamic steady state (see main text and Methods for details). Two sets of three simulations were run, with Augmin residence times of 1 or 13 s, as indicated. The MT plus end distributions predicted over time were compared with those measured in metaphase spindles. **(I)** Mean standard error of each prediction. Each data point is the mean measured over 30 s, in individual simulations; lines denote the mean of three simulations over time for each tested residence time. **(J)** Mean MT plus end distributions predicted for the last 30 s of each simulation, compared with the total EB3-EGFP fluorescence measured in Fig. 1 (B and C). Lines and shaded areas denote mean ± SD, respectively. Scale bars, 10 μm. AU, arbitrary units.

Table S1. **Key resources and reagents used in this study, and the respective sources**

Reagent or resource	Source	Identifier
Experimental models: cell lines used in this study		
HeLa Kyoto (WT)	Obtained from S. Narumiya (Kyoto University, Kyoto, Japan)	Lab ID #1
HeLa Kyoto EB3-EGFP/mCherry-CENPA	Cuylen et al., 2016	Lab ID #826
HeLa Kyoto EGFP-α-tubulin/H2B-mCherry	Dick and Gerlich, 2013	Lab ID #157
hTERT-RPE1 RIEP receptor	Samwer et al., 2017	Lab ID #1092
hTERT-RPE1 EB3-EGFP/mCherry-CENPA	This study	Lab ID #1434
HeLa Kyoto EB3-tagRFP	This study	Lab ID #1753
HeLa Kyoto Mad2-EGFP/mCherry-CENPA	Dick and Gerlich, 2013	Lab ID #1156
Plasmids		
Lenti_EGFP-P2A-BAF_IRES_Blast	Samwer et al., 2017	Lab ID #1161
Lenti_EGFP-P2A-HAUS6_IRES_Blast	This study	Lab ID #1758
Lenti_EGFP-P2A-siRNAresHAUS6_IRES_Blast	This study	Lab ID #1759
Lenti_EGFP-P2A_IRES_Blast	This study	Lab ID #1765
pCR-BluntII-TOPO_HAUS6	Mammalian Gene Collection; storage and distribution provided by the PlasmID Repository at Harvard Medical School and funded in part by National Cancer Institute Cancer Center support grant NHI 5 P30 CA06516	PlasmID HsCD00347195, Lab ID #1757
Chemicals		
SiR-Hoechst	Obtained from Kai Johnsson (EPFL, Lausanne, Switzerland; Lukinavičius et al., 2015)	Lab ID #377
SiR-tubulin	Obtained from Kai Johnsson (Lukinavičius et al., 2014)	Lab ID #295
RNAiMAX	Thermo Fisher Scientific	13778-150
Tween 80	Merck (Sigma-Aldrich)	P1754
Oligonucleotides: siRNAs used in this study		
Scrambled control sense: 5′-UUCUCCGAACGUGUCACGUTT-3′	Ambion	s229174 Lab ID #153
HAUS6 sense: 5′-CAGUUAAGCAGGUACGAAATT-3′	Qiagen: HP custom siRNA, unmodified	Lab ID #218
HAUS4 sense: 5′-AGAUUUUGUCCGACACUUATT-3′	Ambion	s29779 Lab ID #213
KATNA1 sense: 5′-GGCUCGAUUUUAUUCUCCATT-3′	Ambion	s21895 Lab ID #269
Antibodies		
Mouse monoclonal anti-actin (used for WB at 1: 10000)	Merck (Millipore)	MAB1501 Lab ID #186
Rabbit monoclonal anti-HAUS6 (used for WB at 1:2,000, for IF at 1:500)	Abcam	AB173281 Lab ID #268
HRP-goat anti-mouse (used for WB at 1:5,000)	Bio-Rad	170-6516 Lab ID #185
HRP-goat anti-rabbit (used for WB at 1:5,000)	Bio-Rad	170-6515 Lab ID #158
Rabbit monoclonal anti–α-tubulin, acetyl K40 (used for IF at 1:1,000)	Abcam	AB179484 Lab ID #315
Mouse monoclonal anti-α-tubulin-FITC (used for IF at 1:1,000)	Merck (Sigma-Aldrich)	F2168 Lab ID #172
Alexa Fluor 594 anti-rabbit (used for IF at 1:1,000)	Molecular Probes	A21207 Lab ID #56
Software and plugins		
ImageJ 1.48h, 64-bit	National Institutes of Health	–
MultiStackReg Fiji plugin	https://github.com/miura/MultiStackRegistration	–
Running ZProjector Fiji plugin	https://imagej.nih.gov/ij/plugins/index.html#more	---
MATLAB R2016a, 64-bit	MathWorks	–
GraphPad Prism 7	GraphPad Software	–
Other		
Nunc Lab-Tek II chambered coverglass	Thermo Fisher Scientific	155409

IF, immunofluorescence; WB, Western blot; –, not applicable.

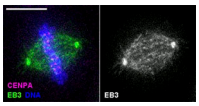

Video 1. **Growing MT plus ends in a live HeLa cell, imaged by spinning disk confocal microscopy.** Representative example of a metaphase cell expressing EB3-EGFP (green) and mCherry-CENPA (magenta). Cells were preincubated with SiR-Hoechst for staining of chromosomes (blue). Selected frames are shown in Fig. 1 A. Spindle morphology and the overall distribution of EGFP-marked plus ends (right) remained constant throughout. Scale bar, 10 µm.

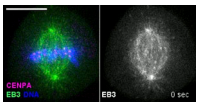

Video 2. **Growing MT plus ends in a live hTERT-RPE1 cell, imaged by spinning disk confocal microscopy.** Representative example of a metaphase cell expressing EB3-EGFP (green) and mCherry-CENPA (magenta). Cells were preincubated with SiR-Hoechst for staining of chromosomes (blue). A selected frame is reproduced in Fig. S1 A. Spindle morphology and the overall distribution of EGFP-marked plus ends (right) remained constant throughout. Scale bar, 10 µm.

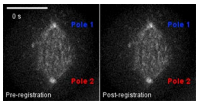

Video 3. **Time-lapse movie registration to correct for spindle rotation.** Individual frames of EB3-EGFP videos were registered by rigid-body transformation before analysis (see Materials and methods for details). Overlay illustrates automatic tracking of spindle poles before and after registration. Scale bar, 10 µm.

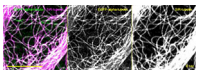

Video 4. **SiR-tubulin labels the lattice of MTs with a delay relative to their polymerization.** HeLa cells expressing EGFP-α-tubulin (green) were incubated with 100nM SiR-tubulin (magenta) and imaged by point-scanning confocal microscopy at 1 s/frame. Images were collected at the bottom surface of interphase cells, in regions of low MT density, to resolve individual MTs as they grow. The first frame is reproduced in Fig. 3 A. Scale bar, 10 µm.

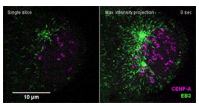

Video 5. **Growing MT plus ends in a live HeLa cell, imaged by 3D Lattice light-sheet microscopy.** Representative example of an early prometaphase cell expressing EB3-EGFP (green) and mCherry-CENPA (magenta). Shown are a selected focal plane (left) and a maximum-intensity projection (right) of a deconvolved video (t = 0, nuclear envelope disassembly). Selected frames of the projection are reproduced in Fig. 5 A. Scale bar, 10 µm.

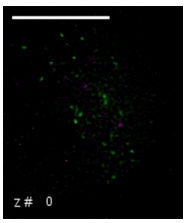

Video 6. **3D stack of prometaphase cell imaged by lattice light-sheet microscopy.** HeLa cell expressing EB3-EGFP (green) and mCherry-CENPA (magenta). Same cell as in Video 5, at t = 150 s after nuclear envelope disassembly. Scale bar, 10 µm.

References

Cuylen, S., C. Blaukopf, A.Z. Politi, T. Müller-Reichert, B. Neumann, I. Poser, J. Ellenberg, A.A. Hyman, and D.W. Gerlich. 2016. Ki-67 acts as a biological surfactant to disperse mitotic chromosomes. *Nature.* 535:308–312. https://doi.org/10.1038/nature18610

Dick, A.E., and D.W. Gerlich. 2013. Kinetic framework of spindle assembly checkpoint signalling. *Nat. Cell Biol.* 15:1370–1377. https://doi.org/10.1038/ncb2842

Lukinavičius, G., L. Reymond, E. D'Este, A. Masharina, F. Göttfert, H. Ta, A. Güther, M. Fournier, S. Rizzo, H. Waldmann, et al. 2014. Fluorogenic probes for live-cell imaging of the cytoskeleton. *Nat. Methods.* 11:731–733. https://doi.org/10.1038/nmeth.2972

Lukinavičius, G., C. Blaukopf, E. Pershagen, A. Schena, L. Reymond, E. Derivery, M. González-Gaitán, E. D'Este, S.W. Hell, D. Wolfram Gerlich, and K. Johnsson. 2015. SiR-Hoechst is a far-red DNA stain for live-cell nanoscopy. *Nat. Commun.* 6:8497. https://doi.org/10.1038/ncomms9497

Samwer, M., M.W.G. Schneider, R. Hoefler, P.S. Schmalhorst, J.G. Jude, J. Zuber, and D.W. Gerlich. 2017. DNA Cross-Bridging Shapes a Single Nucleus from a Set of Mitotic Chromosomes. *Cell.* 170:956–972.e23. https://doi.org/10.1016/j.cell.2017.07.038